

1 Expanded equine cumulus-oocyte complexes exhibit higher meiotic competence and lower glucose
2 consumption than compact cumulus-oocyte complexes

3

4 **Running head:** Equine oocyte glucose metabolomics.

5

6 L. González-Fernández^{A,B}, M.J. Sánchez-Calabuig^C, M.G. Alves^D, P.F. Oliveira^D, S. Macedo^A, A. Gutiérrez-
7 Adán^C, A. Rocha^A, B. Macías-García^{A,E,F}

8

9 ^ACECA/ICETA – Animal Sciences Centre, ICBAS – Abel Salazar Biomedical Institute, University of Porto,
10 Portugal

11 ^BResearch Group of Intracellular Signalling and Technology of Reproduction (SINTREP), School of Veterinary
12 Medicine, University of Extremadura, Cáceres, Spain.

13 ^CDepartment of Animal Reproduction, INIA, Madrid, Spain.

14 ^DDepartment of Microscopy, Cell Biology Laboratory, Abel Salazar Institute of Biomedical Sciences (ICBAS) &
15 Unit for Multidisciplinary Research in Biomedicine (UMIB), University of Porto, Porto, Portugal.

16 ^EAssisted Reproduction Unit, JesúsUsón Minimally Invasive Surgery Centre (CCMIJU), Cáceres, Spain.

17

19 Spain. e-mail: bea_macias@hotmail.com

20

21 **Abstract**

22

23 Equine cumulus-oocyte complexes (COCs) are classified as compact (cCOC) or expanded (eCOC) and vary in
24 their meiotic competence. This divergence could be related to different glucose metabolism. To test this
25 hypothesis eCOCs, cCOCs, and expanded or compact mural granulosa cells (EC and CC respectively) were
26 matured *in vitro* for 30 hours and the maturation rate, glucose metabolism, and expression of genes involved in
27 glucose transport, glycolysis, apoptosis and meiotic competence were determined. Significant differences were
28 found between eCOCs and cCOCs maturation rates (50% vs. 21.7 %; n = 192 and 46 respectively, $p < 0.001$),
29 glucose consumption (1.8 ± 0.5 vs. 27.9 ± 5.9 nmol/COC; mean \pm SEM), pyruvate production (0.1 ± 0.0 vs. $2.4 \pm$
30 0.8 nmol/COC; mean \pm SEM) and lactate production (4.7 ± 1.3 vs. 64.1 ± 20.6 nmol/COC; mean \pm SEM)
31 respectively ($p < 0.05$). Moreover, similar glucose consumption was observed for EC and CC. Hyaluronan
32 binding protein (*TNFAIP6*) expression was increased in eCOCs and EC, solute carrier family 2 (facilitated glucose
33 transporter) member 1 (*SLC2A1*) was increased in eCOCs, while glycolysis-related enzymes and solute carrier
34 family 2 (facilitated glucose transporter) member 3 (*SLC2A3*) expression did not vary between COCs or mural
35 granulosa cell type. Our data demonstrate that metabolic and genomic differences exist between eCOCs and
36 cCOCs and mural granulosa cells in the horse.

37

38 **Additional Keywords:** *in vitro* maturation, glycolysis, nuclear magnetic resonance, horse.

39

40 **Introduction**

41

42 Oocyte *in vitro* maturation (IVM) was achieved for the first time in rabbits by Pincus and Enzmann (1935).
43 Mammalian oocytes can be harvested directly from excised ovaries or removed from the ovaries of live females
44 by transvaginal aspiration (Hinrichs 2010b; Hourvitz *et al.* 2015) and have to reach the metaphase II stage (MII)
45 prior fertilization (Downs 2015). The process of oocyte maturation involves the resumption of meiosis, the
46 expansion of the cumulus cells and the maturation of the cytoplasm (Sutton-McDowall *et al.* 2010). Oocytes are
47 enclosed by numerous layers of granulosa cells which differentiate into two populations spatially and functionally:
48 cumulus cells that surround the oocyte and mural granulosa cells that line the follicular wall; in addition, both

49 granulosa cell lines differ in their metabolism and expression of glycolysis-related genes, establishing a complex
50 interplay with the oocyte (Sugiura *et al.* 2005).

51 A core feature defining the capacity of the individual oocyte to reach MII, also known as meiotic competence, is
52 the initial oocyte quality (Keefe *et al.* 2015). Oocyte quality is generally judged by the appearance of the oocytes
53 under the microscope. Equine oocytes are classified as compact or expanded and are distinguished by the
54 appearance of their cumulus and the degree of expansion of the mural cells present around the COCs (Hinrichs
55 2010b; Gonzalez-Fernandez *et al.* 2015) and their meiotic competence differ vividly; while 71% of expanded
56 oocytes mature in culture, only 21% of compact oocytes (approx.) reach the MII stage (Hinrichs 2010a).

57 Disregarding the species in study, these parameters are subjective. Even when only good quality oocytes are used,
58 the number of mature oocytes and embryos/births obtained will not reach 100% of the initial oocyte pool
59 (Gandolfi and Brevini 2010). In this regard, a lot of effort is being put into identifying factors that define the
60 oocyte meiotic competence including expression and transcription of candidate genes (Mohammadi-
61 Sangcheshmeh *et al.* 2014; Scarlet *et al.* 2016), follicular fluid analysis (Gerard *et al.* 2002; Gérard *et al.* 2014) or
62 oocyte metabolomics (Sessions-Bresnahan *et al.* 2016) among others.

63 Metabolomics allows for the non-invasive study of factors present in the medium that are secreted or consumed as
64 a result of the cumulus-oocyte complex (COC) metabolism (Nel-Themaat and Nagy 2011). Carbohydrate
65 metabolism, namely glucose and pyruvate, deeply influence the meiotic competence of the oocyte in many
66 mammalian species (Downs and Hudson 2000; Herrick *et al.* 2006; Johnson *et al.* 2007; Songsasen *et al.* 2007). In
67 addition, regulation of genes involved in glucose metabolism such as hexokinase (*HK*), phosphofructokinase
68 (*PFK*), pyruvate dehydrogenase (*PDH*) and lactate dehydrogenase (*LDH*) are important for assessing glucose
69 metabolism in any living cell including the oocyte (Kumar *et al.* 2013) and perturbations affecting oocyte's
70 glucose uptake and metabolism impedes meiosis progression (Zheng *et al.* 2007).

71 Herein, we aimed to study the uptake and metabolism of glucose as well as its possible association with the
72 meiotic competence of expanded and compact equine oocytes. To this end, equine expanded (eCOCs) and
73 compact cumulus oocyte-complexes (cCOCs) and mural granulosa cells were cultured separately. After IVM,
74 glucose metabolism was studied by: 1) assessment of glucose consumption and derived metabolites present in the

75 culture medium using nuclear magnetic resonance (NMR) and 2) expression of candidate genes involved in
76 glucose transport, glycolysis, apoptosis and meiotic competence by quantitative polymerase chain reaction
77 (qPCR). In addition, meiosis completion of eCOCs and cCOCs was also assessed by fluorescence microscopy.

78

79 **Materials and methods**

80

81 *Chemicals and reagents*

82

83 All reagents were purchased from Sigma-Aldrich Inc. (Barcelona, Spain) unless otherwise stated.

84

85 *Oocyte harvesting and in vitro maturation*

86 The base medium used for oocyte *in vitro* maturation was Tissue Culture Medium 199 (TCM-199) added with 25
87 mM HEPES (M2520; Sigma, Barcelona, Spain), 25 mM Bicarbonate and 25 µg/ml gentamicin. Bicarbonate was
88 not added when oocytes were handled in the laminar flow hood and the osmolarity was adjusted by NaCl addition.

89 The pH was adjusted to 7.4 and osmolarity was set to 280 mOsm/Kg (approx).

90 Equine ovaries were obtained from a slaughterhouse. The ovaries were placed in a thermic box and transported to
91 the laboratory at room temperature (RT; 20-22°C; 1 hour of transport approx.). Oocytes were obtained by

92 follicular scraping as previously reported (Gonzalez-Fernandez *et al.* 2015). Briefly, each visible follicle was cut
93 with a scalpel blade, meticulously scraped using a bone curette and rinsed on a 35 mm Petri dish with PBS

94 containing 1 U/ml heparin, 25 µg/ml gentamicin and 0.1% polivinilalcohol (PVA). Each follicle was scraped in a
95 separate dish to allow for proper COC and granulosa cell classification. COCs were searched under a dissection
96 microscope, and classified either as cCOC or eCOC based on the morphology of the cumulus and mural granulosa
97 cells observed in the dish; if any signs of expansion were observed, the COC was considered as eCOC while

98 cCOC showed no signs of expansion (Suppl. 1). Twenty microliters of medium containing non-disaggregated

99 mural granulosa cells were aspirated from each of the dishes corresponding to expanded or compact follicles; if

100 expanded and compact cells coexisted in a dish, special care was used to retrieve both. Expanded mural granulosa
101 cells (EC) and compact (CC), cCOCs and eCOCs were then separately transferred to a Petri dish containing TCM-
102 199 added with 10% fetal bovine serum (FBS) until the end of the process. From each dish containing EC and CC
103 two hundred microliters of the pooled granulosa cells were aspirated. COCs and mural granulosa cells were
104 separately held overnight at room temperature ($\approx 22^{\circ}\text{C}$) for a maximum of 16 hours in TCM-199 supplemented
105 with 25 mM bicarbonate and 20% FBS (holding medium or HM) as previously described (Hinrichs 2010b;
106 Martino et al. 2014; Gonzalez-Fernandez et al. 2015). A maximum of 25 oocytes were placed in a 4-well Nunc®
107 plate containing 500 μl HM, filled to the border with mineral oil, sealed using parafilm and wrapped in aluminum
108 foil. The following morning, COCs and mural granulosa cells were transferred to 4-well Nunc® plates containing
109 250 μl of maturation medium covered with mineral oil (TCM supplemented with 25 mM bicarbonate, 5 mU/ml of
110 Follicle stimulating hormone (FSH; Ref. F8174) from sheep pituitary and 10% FBS). The samples were then
111 incubated in a humidified atmosphere of 5% CO_2 in air at 38.5°C for 30 hours. For all the experiments, the
112 maturation medium was allowed to equilibrate for at least 3 hours prior the beginning of the experiment. After
113 oocyte maturation, 200 μl of media of each COC and mural granulosa cell groups were retrieved and stored at -
114 80°C for later nuclear magnetic resonance analysis. All the granulosa cells from EC and CC groups were retrieved
115 and stored at -80°C for protein quantification. A total of 99 eCOCs (15-25 oocytes per well) and 17 cCOCs (1-4
116 oocytes per well) were placed in culture and the supernatants were retrieved for NMR experiments. Sixteen
117 replicates of the IVM experiment were performed for DNA configuration assessment including the oocytes used
118 for NMR; for each replicate, ovaries from 2-5 different mares were used and a total of 192 eCOCs (15-25 oocytes
119 per well) and 46 cCOCs (1-8 oocytes per well) were evaluated.

120

121 *Oocyte degeneration and maturational status evaluation*

122

123 Equine oocytes were evaluated after maturation *in vitro*. First, cumulus cells were removed from the COC with
124 PBS supplemented with 0.2% PVA (PBS+PVA) by meticulous pipetting using decreasing diameter bore glass
125 pipettes (Vitrolife, Götteborg, Sweden) until no granulosa cells were visualized on the zona pellucida. Denuded
126 oocytes were then fixed in 4% formaldehyde in PBS+PVA for 12 hours at 4°C . Then, the oocytes were thoroughly

127 washed in PBS+PVA and stained with 5 µg/ml of Hoechst 33342 at 37°C for 10 minutes in the dark. The oocytes
128 were mounted on slides using glycerol and a coverslip, sealed with nail polish and allowed to air dry. DNA
129 integrity and conformation were classified as follows: germinal vesicle, metaphase I or metaphase II using an
130 Olympus BX41 fluorescence microscope (New Hyde Park, NY, USA using a 40× objective based on previously
131 validated criteria (Hinrichs 2010a)). Oocytes were considered as degenerated when no DNA was present or if
132 unidentifiable chromatin configurations were found.

133

134 *RNA Extraction, reverse transcription and quantification of mRNA transcript abundance*

135

136 Gene expression was analyzed in a) matured eCOCs (n = 30), b) matured cCOCs (n = 21), a representative sample
137 of c) compact mural granulosa cells and d) expanded mural granulosa cells subjected to IVM conditions, retrieved
138 on 4 different days. COCs and granulosa cells were pooled and 7-10 COCs per replicate were used (3 replicates
139 for each COC and mural granulosa cell type).

140 Expanded and compact COCs and mural granulosa cells were processed separately. After IVM, samples were
141 thoroughly washed in PBS+PVA, then placed in 20 µl of RNAlater (Ambion®, Thermo Fisher Scientific Inc.,
142 Oslo, Norway), allowed to equilibrate for 5 min at RT, plunged in liquid nitrogen and stored at -80°C until RNA
143 extraction (Romar *et al.* 2011). Before RNA extraction, samples were thawed and centrifuged at 300 g for 5 min to
144 eliminate the RNA later. Poly (A) RNA was extracted using the Dynabeads® mRNA DIRECT™ Micro Kit
145 (Ambion®, Thermo Fisher Scientific Inc., Oslo, Norway) as previously reported (Bermejo-Alvarez *et al.* 2008). In
146 brief, after samples were incubated in lysis buffer for 10 min with Dynabeads, poly (A) RNA attached to the
147 Dynabeads was magnetically extracted and washed twice with washing buffer A and washing buffer B. RNA was
148 obtained after elution with Tris-HCl. The RT reaction was then performed following the manufacturer's
149 instructions (Epicentre Technologies Corp., Madison, Wis., U.S.A.); to prime the RT reaction and to produce
150 cDNA poly (T) primers, random primers, and MMLV High Performance Reverse Transcriptase enzyme in a total
151 volume of 40 µl were mixed. The tubes containing the mix were heated to 70°C for 5 min to denature the
152 secondary RNA structure and after the addition of 50 units of reverse transcriptase, the RT mix was completed.
153 Retrotranscription was performed by incubating at 25°C for 10 min to favor the annealing of random primers,

154 followed by 37°C for 60 min to allow the RT of RNA, and finally 85°C for 5 min to denature the enzyme. After
155 cDNA synthesis, the samples were diluted to 55 µl in 10 mM Tris –HCl (pH 7.5).

156 Three cDNA samples were used per experimental group and all qPCR reactions were carried out in duplicate in
157 the Rotorgene 6000 Real Time Cyclers™ (Corbett Research, Sydney, Australia). The experiment was conducted
158 to contrast the relative levels of each transcript and the housekeeping gene, histone H2A family, member Z
159 (*H2AFZ*), in each sample. PCR was carried out by adding a 2 µl aliquot of each cDNA sample to the PCR mix
160 (GoTaq qPCR Master Mix, Promega Corporation, Madison, Wis., USA) containing specific primers selected to
161 amplify the selected genes: Tumor necrosis factor alpha-induced protein 6 (TNFAIP6); Growth differentiation
162 factor 9 (*GDF9*); Bone Morphogenetic Protein 15 (*BMP15*); Tumor necrosis factor receptor superfamily, member
163 6 (*FAS*); Fas Ligand (*FASLG*); BCL2-associated X protein (*BAX*), transcript variant X2, mRNA; B-Cell
164 CLL/Lymphoma 2 (*BCL2L1*); solute carrier family 2 (facilitated glucose transporter) member 1 (*SCL2A1*, former
165 *GLUT1*); member 3 (*SCL2A3* former *GLUT3*); Phosphofructokinase, platelet (*PFKP*); Pyruvate dehydrogenase
166 kinase, isozyme 3 (*PDK3*); Lactate dehydrogenase A (*LDHA*); 18 S ribosomal RNA (*RNI8S*); Glyceraldehyde-3-
167 phosphate dehydrogenase (*GAPDH*) and H2A histone family, member Z (*H2AFZ*).

168 Primers were designed using Primer-BLAST software (www.ncbi.nlm.nih.gov/tools/primersblast/) to span exon-
169 exon boundaries when possible. Primer sequences and the approximate sizes of the amplicons are shown in Table
170 1. Cycling conditions were as follows: 94 °C for 3 min followed by 35 cycles of 94°C (15 sec), 56°C (30 sec),
171 72°C (10 sec) and 10 sec for fluorescence acquisition. Each pair of primers was tested to achieve efficiencies
172 close to 1; to quantify their expression levels the comparative cycle threshold C(q) method was used (Schmittgen
173 and Livak 2008). Fluorescence was acquired in each cycle at a temperature higher than the melting temperature of
174 primer dimers to avoid primer artifacts (specific temperatures for each product varied from 80–86 °C). For each
175 sample the threshold cycle or the cycle during the logarithmic linear phase of the reaction at which fluorescence
176 increased above background was determined. The Δ CT value was determined as follows: the endogenous control
177 (*H2AFZ*) C(q) value was subtracted for each sample from each gene C(q) value of the sample. Determination of
178 $\Delta\Delta$ CT involved using the highest sample Δ C(q) value as a constant to subtract from all other Δ C(q) sample values.
179 The equation $2^{-\Delta\Delta CQ}$ was used to determine the fold-changes in the relative gene expression of the target.

180

181 *Nuclear Magnetic Resonance*

182

183 After thawing, the supernatants (200 μ l) of the COCs and mural granulosa cells collected after IVM were
184 subjected to proton nuclear magnetic resonance ($^1\text{H-NMR}$); the $^1\text{H-NMR}$ was run at 14.1 T, 25°C using a 600
185 MHz Bruker Avance spectrometer (Bruker Biospin, Germany), to determine glucose consumption, lactate and
186 pyruvate production as routinely used by our team (Martins *et al.* 2015). Sodium fumarate (final concentration of
187 1 mM) was used as an internal reference (6.50 ppm) to quantify metabolites in solution (multiplet, δ , ppm); lactate
188 (doublet, 1.33); pyruvate (singlet, 2.36); H1- α glucose (doublet, 5.22). Spectra analysis was performed offline.
189 The relative areas of $^1\text{H-NMR}$ resonances were quantified using the curve-fitting routine using the NutsProTM
190 NMR spectral analysis program (Acorn, NMR Inc., Fremont, CA, USA). Results were expressed as metabolite
191 consumption or production per μ g of total protein (pmol/ μ g protein) in EC and CC and as nmol/COC for eCOCs
192 and cCOCs. The NMR spectra for eCOCs and cCOCs were normalized depending upon the number of COCs
193 placed per well and maturation day; 99 eCOCs (15-25 oocytes per well) and 17 cCOCs (1-4 oocytes per well)
194 were placed in culture and their metabolic by-products were analyzed. A total of 7 groups retrieved on 3 different
195 days were analyzed (7 replicates in total).

196

197 *Total protein quantification*

198

199 Total proteins of compact mural granulosa cells (CC) and expanded mural granulosa cells (EC) were isolated
200 using RIPA buffer (PBS, 1% NP-40, 0.5% sodium deoxycholate and 0.1% SDS with freshly added 1 mM
201 phenylmethylsulfonyl fluoride, supplemented with 1% protease inhibitor cocktail, 30 μ l/ml aprotinin and 100 mM
202 sodium orthovanadate). The lysed mural granulosa cells were allowed to stand for 15 minutes on ice, and the
203 suspension was centrifuged at 14000g for 20 minutes at 4°C. The resulting pellet was discarded and protein
204 concentration was determined using the Micro BCATM Protein Assay Kit (Thermo Fisher Scientific) following the

instructions provided by the supplier. The protein concentration obtained was used to normalize the metabolite consumption and production of mural granulosa cells analyzed by NMR.

Statistical analysis

The proportions of oocytes showing different chromatin configurations were compared among groups by Chi-square test with the Yates correction for continuity. The Fisher's Exact Test was used when a value of less than 5 was expected in any treatment. The differences in fold increase expression of the genes under study followed a normal distribution and had homogeneous variances, thus, a student t-test was used to compare pairs of values. When the normality test failed a Mann-Whitney Rank Sum Test was conducted using Sigma Plot software version 11.0. Data obtained by NMR and qPCR were analyzed using the Sigma Stat software package (Jandel Scientific, San Rafael, CA). A Student t-test was performed to study the differences in metabolites between cCOCs and eCOCs and compact and expanded mural granulosa cells; $p < 0.05$ was considered as significant.

Results

Equine oocyte maturation and degeneration rates

Oocyte maturation was evaluated after 30 h in maturation medium. All IVM experiments run in our laboratory from June 2014 to April of 2015 were included (16 IVM experiments in total; 46 cCOCs and 192 eCOCs). Significant differences were found between eCOCs and cCOCs regarding maturation rates (50% vs. 21.7% for eCOCs and cCOCs respectively; $p < 0.001$) and degeneration rates (33.9% vs. 60.9% for eCOCs and cCOCs respectively; $p < 0.001$) after IVM. No significant differences were found between eCOCs and cCOCs for germinal vesicle (GV) or metaphase I (MI) stages ($p > 0.05$; Table 2).

229

230 *Characterization of glucose metabolism in cCOCs and eCOCs, and compact or expanded mural granulosa cells*

231

232 Glucose consumption vividly varied between cCOCs and eCOCs and between compact (CC) and expanded (EC)
233 mural granulosa cells. cCOCs and CC consumed significantly higher amounts of glucose compared to expanded
234 samples (27.9 ± 5.9 vs. 1.8 ± 0.5 nmol/COC, respectively; mean \pm SEM) and EC (40.0 ± 12.0 vs. 0.7 ± 0.0
235 pmol/ μ g protein, respectively; mean \pm SEM) (Fig. 1A). Likewise, cCOCs showed a higher metabolic rate than
236 eCOCs, as pyruvate (2.4 ± 0.8 vs. 0.1 ± 0.0 nmol/COC, cCOCs vs. eCOCs; mean \pm SEM) and lactate production
237 (64.1 ± 20.6 vs. 4.7 ± 1.3 nmol/COC, cCOC vs. eCOC respectively; mean \pm SEM) were greater in cCOCs (Fig.
238 1B and 1C; $p < 0.05$). The same pattern was observed for CC and EC, as pyruvate (5.1 ± 2.7 vs. 0.1 ± 0.0 pmol/ μ g
239 protein, CC vs. EC respectively; mean \pm SEM) and lactate production (42.1 ± 23.7 vs. 2.0 ± 5.0 pmol/ μ g protein,
240 CC vs. EC respectively; mean \pm SEM) were enhanced in CC (Fig. 1B and 1C; $p < 0.05$).

241

242 *Relative mRNA expression of glycolysis, meiotic competence and apoptosis related genes*

243

244 In view of the previously obtained data, the quantitative expression of candidate genes related to apoptosis,
245 glucose metabolism and meiotic competence were compared between eCOCs and cCOCs and between EC and
246 CC. We first studied the gene expression levels of three housekeeping genes (*H2AFZ*, *RNI8S*, and *GAPDH*) to
247 identify the housekeeping with minimal variability under our experimental conditions (compact or expanded
248 COCs, and compact or expanded mural granulosa cells). In our experimental setting *H2AFZ* was the most suitable
249 housekeeping gene for normalizing mRNA levels (data not shown). The expression of this housekeeping gene was
250 found to be directly proportional to the amount of mRNA present in non-normalized reverse transcription
251 reactions; hence, *H2AFZ* was selected for the quantification of the mRNA transcripts. In relation to mRNA
252 expression in COCs, although maturation and degeneration rates were significantly different between cCOCs and

253 eCOCs, only the expression of *TNFAIP6* varied between eCOCs and cCOCs as shown in Fig. 2 (3.17 ± 0.47 vs.
254 1.0 ± 0.60 fold increase; mean \pm SEM; respectively, $p < 0.05$).

255 When the overall expression of the oocyte competence and glucose metabolism related genes were
256 compared between CC and EC only the hyaluronan binding protein (*TNFAIP6*) and the glucose transporter 1
257 (*SLC2A1*) exhibited differences and were consistently enhanced in EC; for *TNFAIP6* (1.0 ± 0.76 vs. 2.13 ± 0.80
258 fold increase; mean \pm SEM respectively, $p < 0.05$) and for *SLC2A1* (1.0 ± 0.69 vs. 16.33 ± 0.79 fold increase;
259 mean \pm SEM respectively, $p < 0.05$). Regarding the apoptosis-related genes, a higher expression was observed in
260 CC compared to EC for *FAS* (4.90 ± 0.92 vs. 1.0 ± 0.36 fold increase; mean \pm SEM respectively, $p < 0.05$) and
261 *BAX/BCL2L1* (2.50 ± 1.25 vs. 0.60 ± 0.20 fold increase; mean \pm SEM respectively, $p < 0.05$) (Fig. 3).

262

263 Discussion

264

265 During the first part of our study, the meiotic competence of eCOCs and cCOCs was assessed and a higher
266 degeneration rate was observed in cCOCs compared to eCOCs after IVM (60.9% vs. 33.9% respectively; $p <$
267 0.05). Previous studies have demonstrated that compact oocytes are retrieved from juvenile follicles and usually
268 degenerate during IVM (65% approx.), while expanded oocytes come from atretic follicles, experience lower
269 degeneration and exhibit higher meiotic competence after IVM ([Hinrichs 2010a](#)). Also, coinciding with previous
270 reports, in our study cCOCs showed lower meiotic competence than eCOCs ([Hinrichs 2010b](#); [Hinrichs 2010a](#)). In
271 view of these data, our maturation and degeneration rates for equine eCOCs and cCOCs are in agreement with the
272 literature and thus, our maturation system is fully validated. In addition, the percentage of eCOCs and cCOCs
273 retrieved in the present study for the NMR and IVM experiments also demonstrate that cCOCs are accurately
274 separated from eCOCs. Although in general cCOCs represent 30% approx. of the COCs retrieved and eCOCs
275 account for 60%, the yield varies between laboratories as the criteria are subjective ([Hinrichs 2010a](#); [Gonzalez-](#)
276 [Fernandez et al. 2015](#)). However, a retrospective study of all the equine follicles scraped from January of 2014 to
277 December of 2015 in our laboratory (1312 oocytes in total) resulted in 326 cCOCs (24%) and 986 expanded
278 (76%) excluding the degenerated oocytes that were discarded and not accounted for (data not shown). These data

279 reflect that, in our setting, the classification criteria are well established and repeatable among oocyte harvesting
280 sessions.

281 Previous studies have demonstrated that the oocytes' glycolytic activity is intimately related to its capacity
282 to resume meiosis (Sutton *et al.* 2003; Sutton-McDowall *et al.* 2010). As denuded oocytes have very poor capacity
283 to metabolize glucose, the granulosa cells surrounding the oocyte are in charge of glucose metabolism (Sutton-
284 McDowall *et al.* 2010) and pyruvate and lactate production during IVM (Donahue and Stern 1968; Billig *et al.*
285 1983). Our data demonstrate that in equine cCOCs and compact mural granulosa cells, glucose consumption and
286 production of pyruvate and lactate are significantly enhanced compared to their expanded counterparts (Fig. 1A,
287 1B and 1C; $p < 0.05$). Interestingly, in contrast with our findings, all the previously mentioned carbohydrates are
288 known to be involved in meiosis resumption of COCs in various species (Downs *et al.* 2002; Downs 2015). For
289 example, glucose plays a key role in nuclear and cytoplasmic maturation of murine COCs (Donahue and Stern
290 1968; Xie *et al.* 2016), pyruvate addition to the IVM medium increases meiosis resumption of bovine and murine
291 COCs (Downs and Hudson 2000; Geshi *et al.* 2000) and lactate is actively produced during IVM of murine COCs
292 (Downs *et al.* 1996). Coinciding with our findings, a brief report has demonstrated that equine cCOCs consume
293 significantly higher amounts of glucose compared to eCOCs but produce lactate at similar rates (Len *et al.* 2016);
294 however, in our study, the compact specimens consistently produced higher lactate quantities (Fig. 1C). This
295 divergence could be due to the different analytical method used (NMR vs. a chemical analyser), to the lower
296 number of COCs used in their study or to the marked differences that exist between laboratories in the equine
297 oocyte classification standards. In addition, in the study by Len *et al.* (2016) insulin-transferrin selenium and
298 significantly higher concentrations of FSH were used (5 mU/ml in the present study vs. 1000 U/ml according to
299 Puregon® manufacturer). It has been demonstrated that both components influence oocytes' glucose metabolism
300 (Janicot and Lane 1989; Downs and Mastropolo 1994), and could also help to explain the apparent divergences
301 found. A limitation of the present study is the lower number of cCOCs used compared to eCOCs but the
302 sensitivity of the technique used (NMR) is high, and has been validated in similar settings (Singh and Sinclair
303 2007). In addition, other reports have also demonstrated different glycolytic capacity of equine COCs depending
304 upon DNA content disregarding their maturational status or the degree of cumulus expansion (Lewis *et al.* 2015).
305 However, clear differences in glucose consumption of eCOCs and cCOCs and mural granulosa cells are reported

306 in the present study. Our data show that compact specimens have higher metabolic activity when compared to
307 eCOCs and expanded mural granulosa cells, but this increased metabolism does not correlate with higher meiotic
308 competence in equine oocytes (Fig. 1 and Table 2). This seems to be species-specific as while, in general, factors
309 such as increased glucose consumption and cumulus compaction are related to improved developmental outcome
310 in human oocytes ([Sutton et al. 2003](#); [Sutton-McDowall et al. 2010](#)), this does not occur in equine oocytes
311 ([Hinrichs 2010a](#)). The finding that cCOCs exhibit higher glucose consumption than eCOCs may agree with the
312 “quiet embryo theory” developed by [Leese \(2002\)](#) who suggested that cell viability is associated with a ‘quiet’
313 metabolism. His theory proposed that the most viable cells exhibit a ‘quieter’ metabolism by regulation of gene
314 expression and changes in the transcriptome and proteome, as they are required to use less energy ([Baumann et al.](#)
315 [2007](#)). Thus, as cCOCs experience a higher degeneration rate, it could be plausible that the higher metabolic rate
316 observed is related to the cCOCs’ attempts to maintain their structures and functions but this hypothesis needs to
317 be further explored.

318 Due to the marked differences found in the parameters studied between expanded and compact specimens, in the
319 next experimental set the relative mRNA expression of genes related to glycolysis, apoptosis and meiotic
320 competence was studied (Table 1). Surprisingly, no differences were observed in the expression of *GDF9* and
321 *BMP15* between eCOCs and cCOCs despite their divergent meiotic competence (Fig. 2). The only developmental
322 competence marker that showed a significant higher expression in eCOCs and EC compared to their compact
323 counterparts was *TNFAIP6*. This gene has been previously described in the equine species and its expression is
324 enhanced by gonadotropins during follicular maturation and ovulation ([Sayasith et al. 2007](#); [Sayasith et al. 2013](#))
325 and depends upon the mare’s age ([Sessions-Bresnahan and Carnevale 2015](#)). The extracellular matrix of equine
326 follicles, as well as COCs, expresses *TNFAIP6* which has been related to cumulus expansion and extrusion of the
327 detached complex during ovulation in the horse ([Sayasith et al. 2007](#)) and influences the meiotic competence of
328 porcine oocytes ([Yuan et al. 2011](#)). Although *GDF9* and *BMP15* have been described to be differently expressed
329 in oocytes of young vs. aged mares ([Campos-Chillon et al. 2015](#)) and mature and immature oocytes, ([Scarlet et al.](#)
330 [2017](#)) no previous reports have been published regarding a possible differential expression in eCOCs and cCOCs.
331 It is widely known that *GDF9* and *BMP15* are involved in cumulus expansion and are related to enhanced meiotic
332 competence ([Kidder and Vanderhyden 2010](#)). However, in the horse *GDF9* and *BMP15* are expressed in the
333 oocyte and not in the cumulus cells ([Scarlet et al. 2017](#)) and their expression varies depending upon the oocyte’s

334 meiosis stage in swine oocytes (Lin *et al.* 2014). In view of these data, our results demonstrate that *TNFAIP6*
335 could be more reliable than *GDF9* or *BMP15* to predict complete cumulus expansion as well as the meiotic
336 competence of pooled equine COCs at different meiotic stages.

337 When the relative abundance of the glycolysis related genes *PFKP*, *PDK3*, *LDHA* and glucose transporters
338 1 and 3 (encoded by *SLC2A1* and *SLC2A3*) was compared between expanded and compact mural granulosa cells,
339 only *SLC2A1* exhibited a significantly increased expression in EC (Fig. 3). The expression of glucose transporter
340 1 (*SLC2A1*) has been shown to dramatically increase in dominant follicles, thecal and granulosa cells undergoing
341 atresia in bovine (Nishimoto *et al.* 2006); in addition, negative correlations between glucose concentrations in
342 follicular fluid and glucose transporter 1 and 3 expression have also been reported (Nishimoto *et al.* 2006). This
343 scenario has been described in glucose-deprived bovine chromaffin cells in which *SLC2A1* and *SLC2A3* were
344 significantly overexpressed (Fladeby *et al.* 2003), implying a local regulatory mechanism of glucose uptake to
345 compensate glucose deprivation. Coincidentally, one of the first signs of follicular atresia is the loss of thecal
346 vascularity and a decrease in the glucose and oxygen supply to the follicles. As previously stated, EE are retrieved
347 from atretic follicles in the horse explaining the higher *SLC2A1* expression and lower glucose consumption
348 compared to CC, which are obtained from juvenile follicles (Hinrichs and Schmidt 2000). The higher expression
349 of apoptosis related genes in CC are in agreement with previous reports in goat oocytes in which granulosa cell
350 expansion inversely correlates with apoptosis after IVM (Han *et al.* 2006). The higher relative abundance of
351 apoptotic-related mRNAs and lower expression of *TNFAIP6* in CC may indicate an incomplete or less-functional
352 expansion explaining why many cCOCs degenerate after IVM (Table 2 and Fig. 2).

353 In conclusion our results demonstrate that compact COCs and mural granulosa cells exhibit higher glucose
354 consumption and lower meiotic competence compared to their expanded counterparts. The relative abundance of
355 *SLC2A1* and *TNFAIP6* is consistently higher in expanded mural granulosa cells while the expression of apoptotic
356 related genes predominates in compact mural granulosa cells. *TNFAIP6* is highly expressed in expanded samples
357 (COCs and mural cells) and could be a more reliable predictor of complete granulosa cell expansion and meiotic
358 competence than *GDF9* and/or *BMP15* in equine pooled COCs. More research is needed to establish if, in order to
359 increase the meiotic competence of equine COCs, the IVM conditions should vary for compact and expanded
360 specimens in view of the vivid metabolic differences observed.

Acknowledgments

This work was financed by AGL2015-66145-R funding from the Spanish Ministry of Economy, Industry and Competitiveness and by AGL2015-73249-JIN(AEI/FEDER/UE) from the "Agencia Estatal de Investigación" (AEI) (Spanish Ministry of Economy, Industry and Competitiveness) and "Fondo Europeo de Desarrollo Regional" (FEDER). Beatriz Macías-García holds a postdoctoral grant "Juan de la Cierva Incorporación"(IJCI-2014-19428) from the Spanish Ministry of Economy, Industry and Competitiveness. L.G.-F. (Grant reference: SFRH/BPD/85532/2012) and B. M.-G. (Grant reference: SFRH/BPD/84354/2012) were also partially funded by Fundação para a Ciência e a Tecnologia (Portuguese Ministry for Science, Technology and Higher Education) co-funded by Programa Operacional Potencial Humano (POPH) financed by European Social Fund (ESF) and Portuguese national funds from Ministry for Science, Technology and Higher Education. The authors thank CECA/ICETA (University of Porto) for funding the abattoir dislocations. The collaboration of Linda Rosa Abattoir is highly appreciated. The authors wish to thank the Laboratory of Applied Physiology (Department of Aquatic Production) of the ICBAS (University of Porto) and especially Mariana Hinzmann for allowing us to use their fluorescence microscope. RNA later was kindly provided by Dr. Michael Jowers.

References

- Baumann, C.G., Morris, D.G., Sreenan, J.M., and Leese, H.J. (2007) The quiet embryo hypothesis: Molecular characteristics favoring viability. *Molecular Reproduction and Development* **74**, 1345-1353
- Bermejo-Alvarez, P., Rizo, D., Rath, D., Lonergan, P., and Gutierrez-Adan, A. (2008) Epigenetic differences between male and female bovine blastocysts produced in vitro. *Physiol Genomics* **32**, 264-72
- Billig, H., Hedin, L., and Magnusson, C. (1983) Gonadotrophins stimulate lactate production by rat cumulus and granulosa cells. *Acta Endocrinol (Copenh)* **103**, 562-566
- Campos-Chillon, F., Farmerie, T.A., Bouma, G.J., Clay, C.M., and Carnevale, E.M. (2015) Effects of aging on gene expression and mitochondrial DNA in the equine oocyte and follicle cells. *Reprod Fertil Dev* **27**, 925-33
- Donahue, R.P., and Stern, S. (1968) Follicular cell support of oocyte maturation: production of pyruvate in vitro. *J Reprod Fertil* **17**, 395-8

- 394 Downs, S.M. (2015) Nutrient pathways regulating the nuclear maturation of mammalian oocytes. *Reproduction,*
395 *Fertility and Development* **27**, 572-582
396
- 397 Downs, S.M., and Hudson, E.D. (2000) Energy substrates and the completion of spontaneous meiotic maturation.
398 *Zygote* **8**, 339-51
399
- 400 Downs, S.M., Humpherson, P.G., and Leese, H.J. (2002) Pyruvate utilization by mouse oocytes is influenced by
401 meiotic status and the cumulus oophorus. *Molecular Reproduction and Development* **62**, 113-123
402
- 403 Downs, S.M., Humpherson, P.G., Martin, K.L., and Leese, H.J. (1996) Glucose utilization during gonadotropin-
404 induced meiotic maturation in cumulus cell-enclosed mouse oocytes. *Mol Reprod Dev* **44**, 121-31
405
- 406 Downs, S.M., and Mastropolo, A.M. (1994) The participation of energy substrates in the control of meiotic
407 maturation in murine oocytes. *Dev Biol* **162**, 154-68
408
- 409 Fladeby, C., Skar, R., and Serck-Hanssen, G. (2003) Distinct regulation of glucose transport and GLUT1/GLUT3
410 transporters by glucose deprivation and IGF-I in chromaffin cells. *Biochim Biophys Acta* **1593**, 201-8
411
- 412 Gandolfi, F., and Brevini, T.A.L. (2010) RFD Award Lecture 2009. In vitro maturation of farm animal oocytes: a
413 useful tool for investigating the mechanisms leading to full-term development. *Reproduction, Fertility and*
414 *Development* **22**, 495-507
415
- 416 Gérard, N., Fahiminiya, S., Grupen, C.G., and Nadal-Desbarats, L. (2014) Reproductive Physiology and Ovarian
417 Folliculogenesis Examined via 1H-NMR Metabolomics Signatures: A Comparative Study of Large and Small
418 Follicles in Three Mammalian Species (*Bos taurus*, *Sus scrofa domesticus* and *Equus ferus caballus*). *OMICS: A*
419 *Journal of Integrative Biology* **19**, 31-40
420
- 421 Gerard, N., Loiseau, S., Duchamp, G., and Seguin, F. (2002) Analysis of the variations of follicular fluid
422 composition during follicular growth and maturation in the mare using proton nuclear magnetic resonance (1H
423 NMR). *Reproduction* **124**, 241-248
424
- 425 Geshi, M., Takenouchi, N., Yamauchi, N., and Nagai, T. (2000) Effects of sodium pyruvate in nonserum
426 maturation medium on maturation, fertilization, and subsequent development of bovine oocytes with or without
427 cumulus cells. *Biol Reprod* **63**, 1730-4
428
- 429 Gonzalez-Fernandez, L., Macedo, S., Lopes, J.S., Rocha, A., and Macias-Garcia, B. (2015) Effect of Different Media
430 and Protein Source on Equine Gametes: Potential Impact During In Vitro Fertilization. *Reprod Domest Anim* **50**,
431 1039-46
432
- 433 Han, Z.B., Lan, G.C., Wu, Y.G., Han, D., Feng, W.G., Wang, J.Z., and Tan, J.H. (2006) Interactive effects of granulosa
434 cell apoptosis, follicle size, cumulus-oocyte complex morphology, and cumulus expansion on the developmental
435 competence of goat oocytes: a study using the well-in-drop culture system. *Reproduction* **132**, 749-58
436
- 437 Herrick, J.R., Brad, A.M., and Krisher, R.L. (2006) Chemical manipulation of glucose metabolism in porcine
438 oocytes: effects on nuclear and cytoplasmic maturation in vitro. *Reproduction* **131**, 289-98
439
- 440 Hinrichs, K. (2010a) The equine oocyte: factors affecting meiotic and developmental competence. *Mol Reprod*
441 *Dev* **77**, 651-61
442
- 443 Hinrichs, K. (2010b) In vitro production of equine embryos: state of the art. *Reprod Domest Anim* **45 Suppl 2**, 3-8
444

- 445 Hinrichs, K., and Schmidt, A.L. (2000) Meiotic Competence in Horse Oocytes: Interactions Among Chromatin
446 Configuration, Follicle Size, Cumulus Morphology, and Season. *Biology of Reproduction* **62**, 1402-1408
447
- 448 Hourvitz, A., Yerushalmi, G.M., Maman, E., Raanani, H., Elizur, S., Brengauz, M., Orvieto, R., Dor, J., and Meirou,
449 D. (2015) Combination of ovarian tissue harvesting and immature oocyte collection for fertility preservation
450 increases preservation yield. *Reprod Biomed Online* **31**, 497-505
451
- 452 Janicot, M., and Lane, M.D. (1989) Activation of glucose uptake by insulin and insulin-like growth factor I in
453 *Xenopus* oocytes. *Proc Natl Acad Sci U S A* **86**, 2642-6
454
- 455 Johnson, M.T., Freeman, E.A., Gardner, D.K., and Hunt, P.A. (2007) Oxidative Metabolism of Pyruvate Is Required
456 for Meiotic Maturation of Murine Oocytes In Vivo. *Biology of Reproduction* **77**, 2-8
457
- 458 Keefe, D., Kumar, M., and Kalmbach, K. (2015) Oocyte competency is the key to embryo potential. *Fertil Steril*
459 **103**, 317-322
460
- 461 Kidder, G.M., and Vanderhyden, B.C. (2010) Bidirectional communication between oocytes and follicle cells:
462 ensuring oocyte developmental competence. *Canadian journal of physiology and pharmacology* **88**, 399-413
463
- 464 Kumar, P., Rajput, S., Verma, A., De, S., and Datta, T.K. (2013) Expression pattern of glucose metabolism genes in
465 relation to development rate of buffalo (*Bubalus bubalis*) oocytes and in vitro-produced embryos.
466 *Theriogenology* **80**, 914-22
467
- 468 Leese, H.J. (2002) Quiet please, do not disturb: a hypothesis of embryo metabolism and viability. *Bioessays* **24**,
469 845-849
470
- 471 Len, J., McDowall, M., Anastasie, M., and Kleeman, D. (2016) Glucose uptake and lactate production of equine
472 cumulus-oocyte complexes during in vitro maturation. *Journal of Equine Veterinary Science* **41**, 59
473
- 474 Lewis, N., Hinrichs, K., Brison, D., Sturmey, R., Grove-White, D., Schnauffer, K., and McGregor-Argo, C. (2015) 184
475 PRELIMINARY FINDINGS ON CARBOHYDRATE METABOLISM OF INTACT EQUINE CUMULUS-OOCYTE COMPLEXES
476 DURING IN VITRO MATURATION. *Reproduction, Fertility and Development* **28**, 223-223
477
- 478 Lin, Z.L., Li, Y.H., Xu, Y.N., Wang, Q.L., Namgoong, S., Cui, X.S., and Kim, N.H. (2014) Effects of Growth
479 Differentiation Factor 9 and Bone Morphogenetic Protein 15 on the in vitro Maturation of Porcine Oocytes.
480 *Reproduction in Domestic Animals* **49**, 219-227
481
- 482 Martino, N.A., Dell'Aquila, M.E., Filioli Uranio, M., Rutigliano, L., Nicassio, M., Lacalandra, G.M., and Hinrichs, K.
483 (2014) Effect of holding equine oocytes in meiosis inhibitor-free medium before in vitro maturation and of
484 holding temperature on meiotic suppression and mitochondrial energy/redox potential. *Reprod Biol Endocrinol*
485 **12**, 99
486
- 487 Martins, A.D., Moreira, A.C., Sa, R., Monteiro, M.P., Sousa, M., Carvalho, R.A., Silva, B.M., Oliveira, P.F., and
488 Alves, M.G. (2015) Leptin modulates human Sertoli cells acetate production and glycolytic profile: a novel
489 mechanism of obesity-induced male infertility? *Biochim Biophys Acta* **1852**, 1824-32
490
- 491 Mohammadi-Sangcheshmeh, A., Held, E., Rings, F., Ghanem, N., Salilew-Wondim, D., Tesfaye, D., Sieme, H.,
492 Schellander, K., and Hoelker, M. (2014) Developmental competence of equine oocytes: impacts of zona pellucida
493 birefringence and maternally derived transcript expression. *Reproduction, Fertility and Development* **26**, 441-452
494

- 495 Nel-Themaat, L., and Nagy, Z.P. (2011) A review of the promises and pitfalls of oocyte and embryo
496 metabolomics. *Placenta* **32 Suppl 3**, S257-63
497
- 498 Nishimoto, H., Matsutani, R., Yamamoto, S., Takahashi, T., Hayashi, K.-G., Miyamoto, A., Hamano, S., and
499 Tetsuka, M. (2006) Gene expression of glucose transporter (GLUT) 1, 3 and 4 in bovine follicle and corpus
500 luteum. *Journal of Endocrinology* **188**, 111-119
501
- 502 Pincus, G., and Enzmann, E.V. (1935) The Comparative Behavior of Mammalian Eggs in Vivo and in Vitro : I. The
503 Activation of Ovarian Eggs. *J Exp Med* **62**, 665-75
504
- 505 Romar, R., De Santis, T., Papillier, P., Perreau, C., Thelie, A., Dell'Aquila, M.E., Mermillod, P., and Dalbies-Tran, R.
506 (2011) Expression of maternal transcripts during bovine oocyte in vitro maturation is affected by donor age.
507 *Reprod Domest Anim* **46**, e23-30
508
- 509 Sayasith, K., Dore, M., and Sirois, J. (2007) Molecular characterization of tumor necrosis alpha-induced protein 6
510 and its human chorionic gonadotropin-dependent induction in theca and mural granulosa cells of equine
511 preovulatory follicles. *Reproduction* **133**, 135-45
512
- 513 Sayasith, K., Lussier, J., Doré, M., and Sirois, J. (2013) Human chorionic gonadotropin-dependent up-regulation of
514 epiregulin and amphiregulin in equine and bovine follicles during the ovulatory process. *General and*
515 *Comparative Endocrinology* **180**, 39-47
516
- 517 Scarlet, D., Ille, N., Ertl, R., Alves, B.G., Gastal, G.D., Paiva, S.O., Gastal, M.O., Gastal, E.L., and Aurich, C. (2016)
518 Glucocorticoid metabolism in equine follicles and oocytes. *Domest Anim Endocrinol* **59**, 11-22
519
- 520 Scarlet, D., Ille, N., Ertl, R., Alves, B.G., Gastal, G.D.A., Paiva, S.O., Gastal, M.O., Gastal, E.L., and Aurich, C. (2017)
521 Glucocorticoid metabolism in equine follicles and oocytes. *Domestic Animal Endocrinology* **59**, 11-22
522
- 523 Schmittgen, T.D., and Livak, K.J. (2008) Analyzing real-time PCR data by the comparative C(T) method. *Nat Protoc*
524 **3**, 1101-8
525
- 526 Sessions-Bresnahan, D.R., and Carnevale, E.M. (2015) Age-associated changes in granulosa cell transcript
527 abundance in equine preovulatory follicles. *Reproduction, Fertility and Development* **27**, 906-913
528
- 529 Sessions-Bresnahan, D.R., Schauer, K.L., Heuberger, A.L., and Carnevale, E.M. (2016) Effect of Obesity on the
530 Preovulatory Follicle and Lipid Fingerprint of Equine Oocytes. *Biol Reprod* **94**, 15, 1-12
531
- 532 Singh, R., and Sinclair, K.D. (2007) Metabolomics: Approaches to assessing oocyte and embryo quality.
533 *Theriogenology* **68**, S56-S62
534
- 535 Songsasen, N., Spindler, R.E., and Wildt, D.E. (2007) Requirement for, and patterns of, pyruvate and glutamine
536 metabolism in the domestic dog oocyte in vitro. *Mol Reprod Dev* **74**, 870-7
537
- 538 Sugiura, K., Pendola, F.L., and Eppig, J.J. (2005) Oocyte control of metabolic cooperativity between oocytes and
539 companion granulosa cells: energy metabolism. *Dev Biol* **279**, 20-30
540
- 541 Sutton-McDowall, M.L., Gilchrist, R.B., and Thompson, J.G. (2010) The pivotal role of glucose metabolism in
542 determining oocyte developmental competence. *Reproduction* **139**, 685-95
543

544 Sutton, M.L., Gilchrist, R.B., and Thompson, J.G. (2003) Effects of in-vivo and in-vitro environments on the
 545 metabolism of the cumulus-oocyte complex and its influence on oocyte developmental capacity. *Hum Reprod*
 546 *Update* **9**, 35-48

547
 548 Xie, H.-L., Wang, Y.-B., Jiao, G.-Z., Kong, D.-L., Li, Q., Li, H., Zheng, L.-L., and Tan, J.-H. (2016) Effects of glucose
 549 metabolism during in vitro maturation on cytoplasmic maturation of mouse oocytes. *Sci Rep* **6**, 20764

550
 551 Yuan, Y., Ida, J.M., Paczkowski, M., and Krisher, R.L. (2011) Identification of developmental competence-related
 552 genes in mature porcine oocytes. *Molecular Reproduction and Development* **78**, 565-575

553
 554 Zheng, P., Vassena, R., and Latham, K.E. (2007) Effects of in vitro oocyte maturation and embryo culture on the
 555 expression of glucose transporters, glucose metabolism and insulin signaling genes in rhesus monkey oocytes
 556 and preimplantation embryos. *Mol Hum Reprod* **13**, 361-71

557
 558
 559

560 **Figure legends**

561
 562 **Fig. 1** Glucose consumption in compact cumulus oocyte complexes (cCOCs); expanded cumulus oocyte
 563 complexes (eCOCs); compact mural granulosa cells (CC) and expanded mural granulosa cells (EC). Glucose
 564 consumption (1A); pyruvate (1B) and lactate production (1C) by cCOCs, eCOCs, CC and EC. For this experiment
 565 116 COCs were used: 17 cCOCs and 99 eCOCs. For COCs, values are expressed as nmol/COC; for mural cells
 566 values are expressed as pmol/μg protein. Data are presented as the mean percentage ± SEM. A student t-test was
 567 used to compare a pair of values; statistical significance was set at * p < 0.05.

568
 569 **Fig. 2** Relative mRNA expression of genes related to oocyte's meiotic competence, apoptosis and glucose
 570 metabolism in compact cumulus oocyte complexes (cCOCs) and expanded cumulus oocyte complexes (eCOCs).
 571 The relative abundance of the candidate genes related to meiotic competence (*TNFAIP6*, *GDF9*, *BMP15*),
 572 apoptosis (*FAS*, *BAX*, *BCL2L1*) and glucose metabolism (*SCL2A1*, *SCL2A3*, *PFKP*, *PKD3*, *LDHA*) was compared
 573 between cCOCs and eCOCs after IVM. Bars represent the mean of 5 different replicates and the error bar show
 574 the standard error of the mean. A student t-test or Mann-Whitney Rank Sum Test was used to compare pairs of
 575 values; statistical significance was set at * p < 0.05.

576

577 **Fig. 3** Relative mRNA expression of genes related to oocyte's meiotic competence, apoptosis and glucose
578 metabolism in compact mural granulosa (CC) and expanded mural granulosa (EC). The relative mRNA expression
579 of the candidate genes related to oocyte competence (*TNFAIP6*), apoptosis (*FAS*, *FASLG*, *BAX*, *BCL2L1*) and
580 glucose metabolism (*SCL2A1*, *SCL2A3*, *PFKP*, *PDK3*, *LDHA*) in CC and EC was compared after IVM. Bars
581 represent the mean of 3 different replicates and the error bar shows the standard error of the mean. A student t-test
582 or Mann-Whitney Rank Sum Test was used to compare pair of values; statistical significance was set at * $p < 0.05$.

583

584 **Suppl. File 1** Classification of equine COCs obtained by follicular scraping. Equine follicles were scraped and the
585 cells present in the Petri dish as well as the COCs were carefully evaluated. If any signs of expansion were found
586 in the dish or cumulus, the oocytes were classified as expanded. A) compact COC; B) and C) expanded COCs.
587 The micrographs shown were obtained at 20 x.

588

589

590

591

592

593

594

595

596

597

598

599

600 **Table 1. Gene symbols, accession numbers, primer sequences and amplicon product length for the target**
601 **genes examined**

Entrez gene symbol	Gene name	Accession no.	Primer sequence (5'–3')
<i>BAX</i>	BCL2 associated X, apoptosis regulator	XM_014729721.1	Forward:CCAGGATGCGTCCACCAAGAAG Reverse:GCCCACCTTGAGCACCAATTG
<i>BMP15</i>	Bone morphogenetic protein 15	XM_001496223.2	Forward:GTGAAGCCCTTGACCAATGT Reverse:AGGTGAAGTTGATGGCGGTA
<i>FAS</i>	Tumour necrosis factor receptor superfamily, member 6	XM_005602380.1	Forward:TTACGTGCAAACATGGGATCA Reverse:TCCGGATCCTTCTCTGCATT
<i>FASLG</i>	Fas ligand	NM_001166039.1	Forward:GCTGGTTGTTGCAGGACTGA Reverse:TCAATGACACCGGGCTGTAC
<i>GAPDH</i>	Glyceraldehyde-3-phosphate dehydrogenase	NM_001163856	Forward:ATGGTGAAGTTCGGAGTAAAC Reverse:TGTAGACCATGTAGTTGAGGTCA
<i>GDF9</i>	Growth differentiation factor 9	XM_001504427.2	Forward:GACTTGAGTAAGTGTCCACAGCA Reverse:CAGAGGCCACCTCTACAACAC
<i>H2AFZ</i>	H2A histone family, member Z	NM_174809	Forward:AGGACGACTAGCCATGGACGTGTG Reverse:CCACCACCAGCAATTGTAGCCTTG
<i>LDHA</i>	Lactate dehydrogenase A	NM_001144880.1	Forward:CCGTGTTATCGGAAGTGGTTGC Reverse:AGAATCTCCATGCTCCCAAGG
<i>PDK3</i>	Pyruvate dehydrogenase kinase, isozyme 3	XM_005614047.1	Forward:CAGAGAACCCAGAGATGCTTCA Reverse:AGCTTAGAATCCTGGGGAGGT
<i>PFKP</i>	Phosphofructokinase, platelet	XM_005606965.1	Forward:AAGAACGTGCTGGGCCACATG Reverse:TTCGTGGTGATCCATTGCATGG
<i>SLC2A1</i>	Solute carrier family 2 member 1	NM_001163971.1	Forward:CACTGGAGTCATCAACGCC Reverse:CCACGATCAGCATCTCAAAG
<i>RN18S</i>	18SrRNA	NR_046271.1	Forward:AGAAACGGCTACCACATCCAA Reverse:CCTGTATTGTTATTTTTTCGTCACCTACCT
<i>SLC2A3</i>	Solute carrier family 2 member 3	XM_001498757.2	Forward:GGAGACCACCACCAATGTCTAAGC Reverse:TCCTGGGTTACAACCTGATGAGG
<i>TNFAIP6</i>	Tumour necrosis factor alpha induced protein 6	NM_001081906.1	Forward:GAAGGCGGTGTGTGAATACGA Reverse:GGCTTACAATGGGGTATCCA

602

603

604

605 **Table 2. Chromatin configuration after IVM**

606 Values show the total number of oocytes in each group, with percentages in parentheses. Within
607 columns, values with different superscript letters differ significantly ($P < 0.001$). GV, germinal vesicle;
608 DEG, degenerated

Oocyte type	GV (%)	MI (%)	MII (%)	DEG (%)	Total no. oocytes
Compact oocytes	5 (10.9)	3 (6.5)	10 (21.7) ^a	28 (60.9) ^a	46
Expanded oocytes	21 (10.9)	10 (5.2)	96 (50.0) ^b	65 (33.9) ^b	192

609

610

Figure 1A

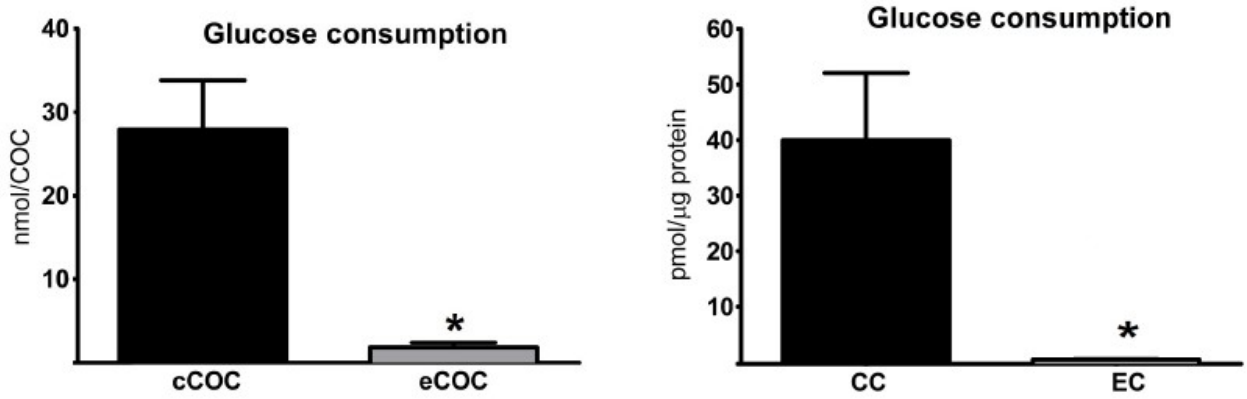


Figure 1B

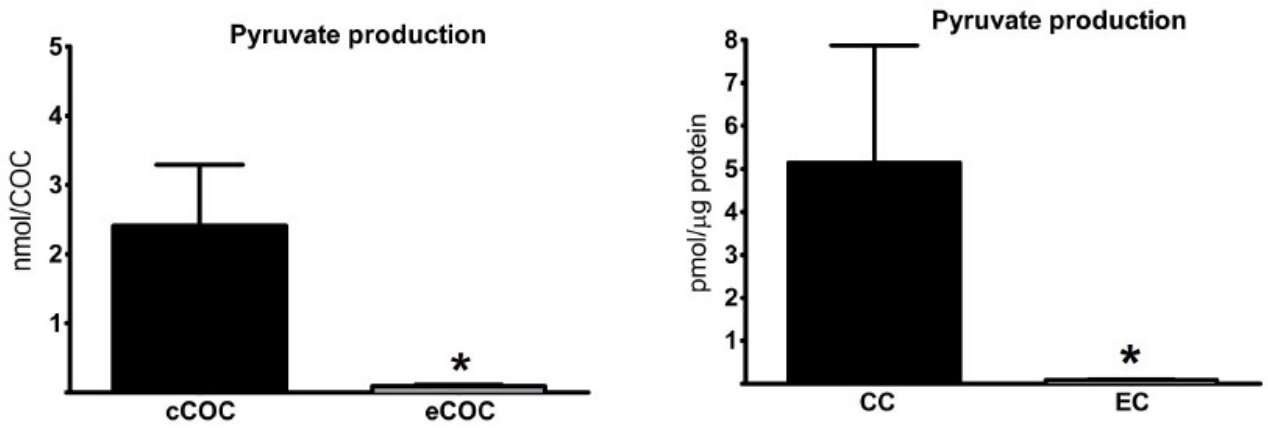


Figure 1C

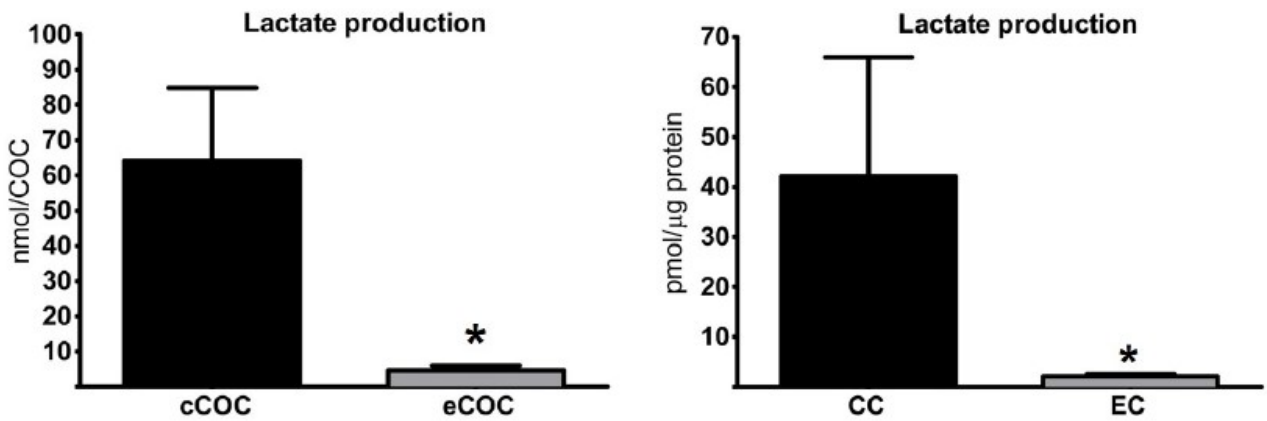
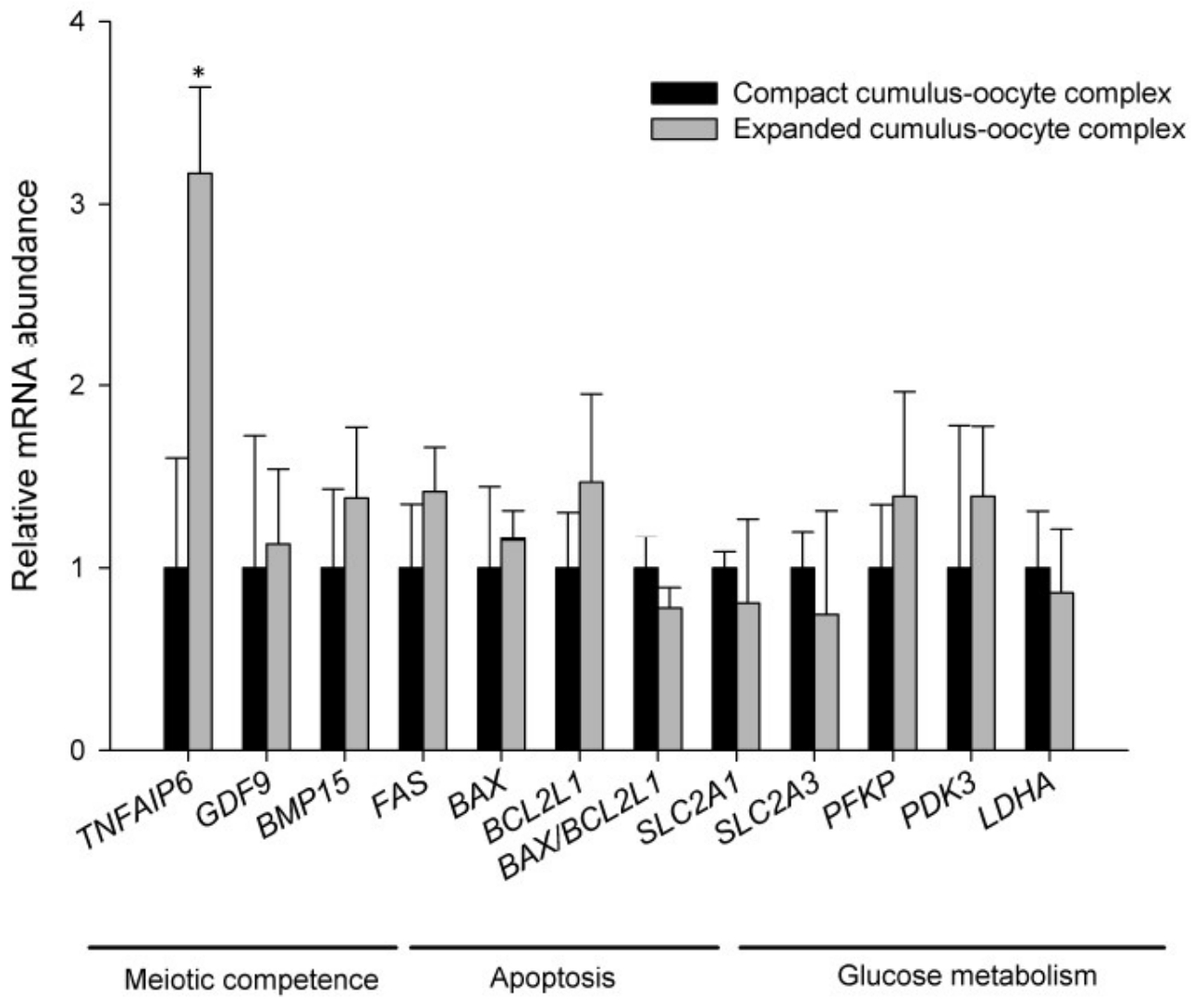


Figure 2



612

613

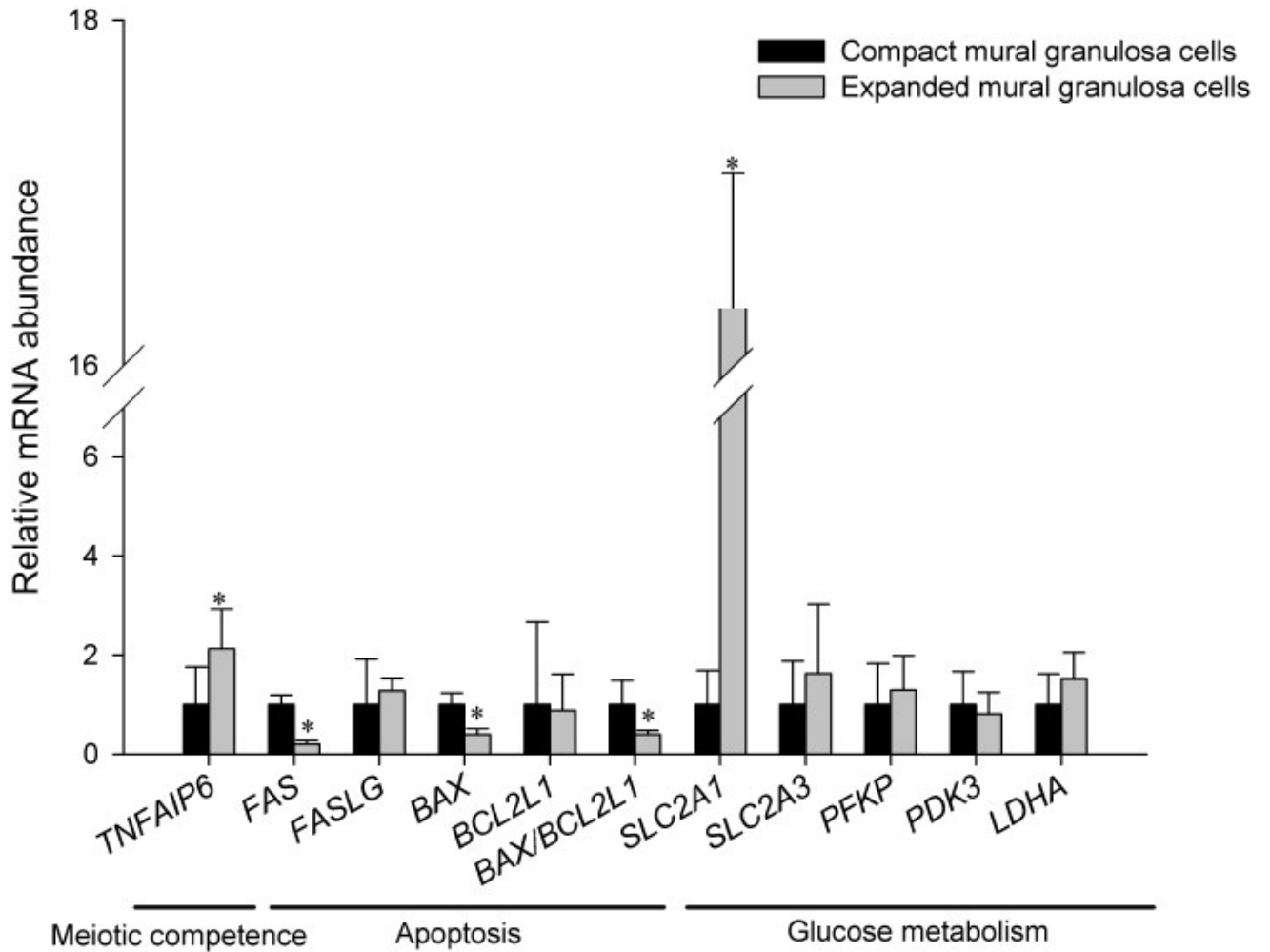
614

615

616

617

Figure 3



618

619

620

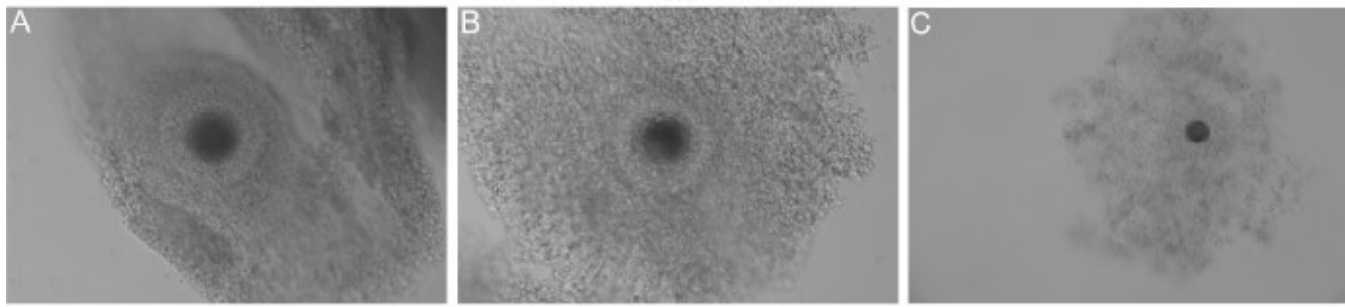
621

622

623

624

Suppl. File 1



625

626

627

628

629

630

631

632

633